Differentiation 111 (2020) 70–78

Contents lists available at ScienceDirect

Differentiation

journal homepage: www.elsevier.com/locate/diff

A crucial role of fibroblast growth factor 2 in the differentiation of hair follicle stem cells toward endothelial cells in a STAT5-dependent manner

Bingjie Cai[a], Yunpeng Zheng[a], Xiaojun Liu[b], Jiadi Yan[a], Junmin Wang[c], Guangwen Yin[a,*]

[a] The First Affiliated Hospital of Zhengzhou University, Zhengzhou, 450052, PR China
[b] Henan Province Medical Instrument Testing Institute, Zhengzhou, 450000, PR China
[c] College of Basic Medical Sciences, Zhengzhou University, Zhengzhou, 450000, PR China

ARTICLE INFO

Keywords:
Fibroblast growth factor 2
Signal transducer and activator of transcription 5
Hair follicle stem cells
Endothelial cells
Cell differentiation

ABSTRACT

Fibroblast growth factor (FGF2) is reported to affect the proliferation, differentiation, and survival abilities of stem cells. In this study, we hypothesize that FGF2 might promote the differentiation of hair follicle stem cell (HFSCs) into endothelial cells (ECs), in a manner dependent on STAT5 activation. We first treated human HFSCs with recombinant human FGF2 to determine the involvement of FGF2 in the differentiation of HFSCs. Then the expression of EC-specific markers including von Willebrand factor (vWF), VE-cadherin, CD31, FLT-1, KDR and Tie2 was evaluated using immunofluorescence and flow cytometry, while the expression of HFSC-specific markers such as K15, K19, Lgr5, Sox9 and Lhx2 was determined by flow cytometry. Next, *in vitro* tube formation was performed to confirm the function of FGF2, and low-density lipoprotein (LDL) uptake by ECs and HFSCs was studied by Dil-acetylated LDL assay. In addition, we transduced FGF2-treated HFSCs with constitutive-active or dominant-negative STAT5A adenovirus vectors. FGF2 up-regulated the expression of EC-specific markers, and promoted the differentiation of HFSCs into ECs, tube formation and LDL uptake. The phosphorylated STAT5 was translocated into the nucleus of HFSCs after FGF2 treatment, but this translocation was blocked by the dominant-negative STAT5A mutant. FGF2 increased the differentiation potential through the activation of STAT5 *in vivo*. Taken together, we find that FGF2 promotes the differentiation of HFSCs into ECs *via* activated STAT5, which gives a new perspective on the role of FGF2 in the development of ischemic vascular disease.

1. Introduction

Hair follicle stem cells (HFSCs) originate from the early committed placode epithelium prior to appearance of the bulge (Woo and Oro, 2011). HFSCs are identified as one of the effective donor cell sources for regenerative medicine because of their strong proliferation ability and multipotency (Zhang et al., 2016). Owing to their excellent proliferation and growth potential, HFSCs have been indicated as a feasible source to induce re-epithelialization and dermal structural regeneration, which are beneficial for skin wound healing (Heidari et al., 2016). As shown in a previous study, the bulge region-derived HFSCs can be differentiated into various cell types, including hair follicle structures, interfollicular epidermis and corneal epithelial cells (Call et al., 2018). Furthermore, HFSCs can be differentiated into vascular endothelial cells (ECs), thereby inducing angiogenesis, which may come to represent a significant breakthrough in the treatment of ischemic diseases (Quan et al., 2017).

Fibroblast growth factors (FGFs) form a family consisting of 18 mammalian fibroblast growth factors, which modulate a plethora of development processes, tissue homeostasis, and metabolic activity, and which present therapeutic targets due to their mitogenic and cytoprotective functions as well as angiogenic potential (Beenken and Mohammadi, 2009; Goetz and Mohammadi, 2013). The FGF family member fibroblast growth factor 2 (FGF2), also known as basic fibroblast growth factor (bFGF), can act as a differentiation inducer and regulatory factor for neural repair to stimulate proliferation and differentiation of neural stem cells (Grigg et al., 2019). Moreover, it is reported that vascular endothelial growth factor (VEGF) and FGFs can together enhance the potential that human HFSCs to differentiate into ECs (Xu et al., 2014). FGF2 has the property of acting as an inducer of angiogenesis (Seo et al., 2016). Interestingly, FGF2 transmits its signals by binding to its receptor FGFR1, thus promoting differentiation, proliferation, and migration of ECs (Chamorro-Jorganes et al., 2014). Therefore, we proposed a hypothesis that FGF2 is likely to stimulate

* Corresponding author. Department of Dermatology, The First Affiliated Hospital of Zhengzhou University, No. 1, Jianshe East Road, Zhengzhou, 450001, Henan Province, PR China.
E-mail address: gwyin67@126.com (G. Yin).

https://doi.org/10.1016/j.diff.2019.10.004
Received 5 July 2019; Received in revised form 21 October 2019; Accepted 23 October 2019
Available online 25 October 2019

differentiation of HFSCs into ECs.

Signal transducer and activator of transcription (STAT) proteins play a dual role as signal transduction molecules in the cytoplasm and as transcription factors, acting upon translocation to the nuclear compartment (Gianti and Zauhar, 2015). Signal transducer and activator of transcription-3 (STAT3), a downstream factor of FGFs, plays a significant role in cell-cycle progression and differentiation (Nichane et al., 2010). An earlier study suggested that STAT5 activation is of vital importance to maintain leukemic stem cells (Tam et al., 2013). Besides, STAT5 activation induced by FGF2 and FGF8b in mouse brain ECs has been previously reported to stimulate EC migration and invasion (Yang et al., 2012). In the current study, we intended to investigate how the differentiation of HFSCs into ECs is regulated by FGF2, finding STAT5 activation is required for FGF2-mediated differentiation. Thus, we have described a novel role for FGF2 in controlling differentiation of HFSCs into ECs and the underlying involvement of STAT5.

2. Materials and methods

2.1. Ethics statement

The animal experiments were performed in strict accordance with the recommendations in the Guide for the Care and Use of Laboratory Animals of the National Institutes of Health. The protocol was approved by the Animal Ethics Committee of The First Affiliated Hospital of Zhengzhou University.

2.2. Cell culture and treatment

Human HFSCs (hHFSCs) and human umbilical vein endothelial cells (hUVECs) were both purchased from Beijing Jing-Meng Stem Cell Technology Co., Ltd. (Beijing, China). HFSCs were cultured in minimum essential medium (MEM; Sigma-Aldrich, St Louis, MO, USA) containing 10% fetal bovine serum (FBS; Invitrogen, Carlsbad, CA, USA) or endothelial cell growth medium-2 (EGM-2; Lonza, Walkersville, MD, USA) containing 2% FBS, namely basal medium (BM). The cells were allocated into a mock group (hHFSCs cultured with MEM), BM group (negative control group, hHFSCs cultured with BM), EC group (positive control group, hUVECs cultured with BM), and FGF2 group (hHFSCs cultured with BM supplemented with FGF2). In the FGF2 group, the BM was supplemented with 10 ng/mL recombinant human FGF2 (Sigma-Aldrich, St. Louis, MO, USA). All the cells were cultured in a humidified environment with 5% CO_2 at 37 °C. The medium was changed every two days, and after seven days, the cell morphology was observed using an optical microscope (Nikon, Tokyo, Japan).

2.3. Adenoviral vector construction and infection

pRK-mSTAT5AHS-Flag, which contains a constitutive-active STAT5A mutant (STAT5A-CA), and pRK-mSTAT5A713-Flag, which contains a dominant-negative STAT5A mutant (STAT5A-DN), were obtained from the Fred Hutchinson Cancer Research Center (Seattle, WA, USA). Both Flag-tagged STAT5A mutants were subcloned separately into the pDNR-1r vector (Clon-tech Laboratories, Inc., PaloAlto, CA, USA) to construct pDNR-1r-mSTAT5AHS-Flag and pDNR-1r-mSTAT5A713-Flag plasmids. Recombinant Adeno-X-viral DNAs were produced with the two STAT5A plasmids and the Cre BD Adeno-X LP vector using the Adeno-XTM Adenoviral Expression System 2 (Becton Dickinson, Franklin Lakes, NJ, USA). Then, the recombinant adenovirus plasmid was transfected into 293 cells using the FuGene6 reagent (Roche, Basle, Switzerland). HFSCs were inoculated into 10-cm culture dishes (5×10^5 cells/well), and infected with the adenovirus. HFSCs contained recombinant human FGF2 after infection for 24 h. The HFSCs were assigned into FGF2 + STAT5A-CA group (where HFSCs were transduced with recombinant pRKmSTAT5AHSFlag vector for 24 h before treatment with FGF2), FGF2 + STAT5A -DN group (where HFSCs were transduced with recombinant pRKmSTAT5A713Flag vector for 24 h before treatment with FGF2), and FGF2 + NC group (where HFSCs were transduced with empty adenovirus vector as control for 24 h before treatment with FGF2). The infection efficiency was measured by Western blot analysis (Yang et al., 2009).

2.4. In vitro tube formation assay

The tube formation assay was conducted according to prior procedures, with some modifications (Kim et al., 2015). Cells were suspended in the medium containing 2% FBS and seeded in 24-well plates containing ice-cold Matrigel solution (Phenol Red-Free; BD Biosciences, USA) at an initial density of 1.5×10^5 cells/1 mL/well. Cell attachment was achieved through pre-incubation at 37 °C for 30 min. Then, the tube formation was monitored in real time with a cell recorder (NanoEntek, Seoul, Korea).

2.5. Dil-acetylated LDL

To evaluate LDL uptake, cells were incubated with diluted acetylated LDL-conjugated Dil-acetylated LDL (10 μg/mL; Molecular Probes, Biomedical Technologies, Stoughton, MA, USA). After being washed three times with probe-free medium, cells were incorporated with fluorochrome-labelled LDL and observed under a microscope (Eclipse E400 Epi-Fluorescence Microscope; Nikon, Japan).

2.6. Immunofluorescence

Cells or tissue sections were washed with phosphate buffered saline (PBS). After PBS washing, the cells were fixed in 4% paraformaldehyde for 15 min. Subsequently, the cells were permeabilized with 0.1% Triton X-100 for 10 min. After final PBS washing, the cells were cultured with 3% bovine serum albumin (BSA) for 30 min. After incubation with primary antibodies against vWF (ab6994, 1:400), VE-cadherin (ab33168, 1:1000), CD31 (ab28364, 1:20), STAT5 (ab16276, 1:1000), p-STAT5 (ab98338, 1:1000), K15 (ab62335, 1:500) for 24 h at 4 °C, the cells were washed three times with PBS. All antibodies used above were purchased from Abcam Inc. (Cambridge, MA, UK). We then applied fluorescein isothiocyanate (FITC)-conjugated goat anti-rabbit secondary antibody (Millipore, Billerica, MA, USA). The nuclei were stained with propidium iodide, and the fluorescence intensity was visualized under a fluorescence microscope (Nikon, Tokyo, Japan), with the cells not exposed to primary antibody serving as controls.

2.7. Flow cytometry

Forty-eight hours after transfection, the cells were collected and centrifuged at $500 \times g$ for 5 min in an Allegra 64R centrifuge (Beckman Coulter, Brea, CA, USA). The pellet was resuspended in PBS/1% BSA. Afterwards, the cells were probed with antibodies against vWF (ab6994, 1:1000), VE-cadherin (ab166715, 1:400), CD31 (ab32457, 1:100), FLT-1 (ab9540), KDR (ab2349), Tie2 (ab24859), K15 (ab80522), K19 (ab52625), Lgr5 (ab75732), Sox9 (ab185230) and Lhx2 (ab140614) respectively on a shaking table (Thermo Scientific, Logan, UT, USA) at room temperature for 30 min. All antibodies were purchased from Abcam Inc. (Cambridge, MA, UK). The cells were then incubated with FITC-conjugated secondary antibody in PBS/1% BSA on the shaking table at room temperature for 30 min. Non-specific staining was determined using FITC-conjugated isotype-matched immunoglobulin (IgG). Fluorescence was detected using a flow cytometer (Becton Dickinson, San Jose, CA, USA) and data were analyzed using a CellQuest software (Becton Dickinson, San Jose, CA, USA).

2.8. RNA isolation and quantitation

In this study, 24 h after transfection, the total RNA was extracted

Table 1
Primer sequences for RT-qPCR.

Target gene	Primer sequence
vWF	F: 5′-TGAAGTATGCGGGCAGCC-3 R: 5′-GCGGTCGATCTTGCTGAAG-3′
VE-cadherin	F: 5′-GCCAGGTATGAGATCGTGGT-3′ R: 5′-GTGTCTTCAGGCACGACAAA-3′
CD31	F: 5′-CCTGCGGTATTCAAAGACAA-3′ R: 5′-GGACATTTCCACTGGCATCT-3′
STAT5	F: 5′-GCAGAGTCCGTGACAGAGG-3′ R: 5′-CCACAGGTAGGGACAGAGTCT-3′
GAPDH	F: 5′-GGAGCGAGATCCCTCCAAAAT-3′ R: 5′-GGCTGTTGTCATACTTCTCATGG-3′

Note: RT-qPCR, reverse transcription quantitative polymerase chain reaction; vWF, von willebrand factor; STAT5, Signal transducer and activator of transcription 5; GAPDH, glyceraldehyde-3-phosphate dehydrogenase.

with Trizol kit (Invitrogen, Carlsbad, CA, USA), and 20 μL portions were reversely transcribed into cDNA using a reverse transcription kit (RR047A, Takara, Kyoto, Japan). Subsequently, PCR was conducted using the SYBR Premix EX Taq kit (RR420A, Takara) on a real-time fluorescence quantitative PCR instrument (ABI7500, ABI, Foster City, CA, USA). The primers for von Willebrand factor (vWF), VE-cadherin, CD31, STAT5 and glyceraldehyde-3-phosphate dehydrogenase (GAPDH) were synthesized by Sangon Biotech Co., Ltd. (Shanghai, China) (Table 1). With GAPDH as an internal reference, the fold changes were calculated by the relative quantification ($2^{-\Delta\Delta Ct}$ method) (Ayuk et al., 2016).

2.9. Western blot assay

In this study, 48 h after transfection, the cells or mouse tissue sections were lysed on ice for 10 min. The protein was quantified by a bicinchoninic acid (BCA) quantitative kit (MultiSciences Biotech Co., Ltd., Hangzhou, Zhejiang, China). After that, the proteins were separated by sodium dodecyl sulfate polyacrylamide gel electrophoresis (SDS-PAGE), transferred to the nitrocellulose membrane, and blocked with 5% BSA in Tris-buffered saline with Tween-20 (TBST) for 60 min, and incubated with primary antibodies at 4 °C overnight. The primary antibodies included STAT5 (ab16276, 1:1000), p-STAT5 (ab32364, 1:1000), Flag (ab106146, 1:1000) and H3 (ab1791, 1:5000). After TBST washing, the membrane was incubated with secondary antibody, horseradish peroxidase-conjugated goat anti-rabbit IgG H & L (ab6721, 1:2000) at room temperature for 2 h. All the above antibodies were purchased from Abcam Inc. (Cambridge, MA, USA). Next, the membrane was washed three times with TBST (20 min each time), followed by the luminescence reaction with a chemiluminescence (ECL) fluorescent detection kit. The relative protein expression was expressed as the ratio of the gray value of the target protein band to that of the internal control protein band using the Quantity One software.

2.10. Preparation of nuclear fractions

Cells were washed two times with cold PBS and then placed into fresh PBS. The cells were then washed rapidly with hypotonic buffer containing 10 mM N-2-hydroxyethylpiperazine-N′-2-ethanesulfonic acid (HEPES; pH = 7.9), 1.5 mM $MgCl_2$, 10 mM KCl, 0.2 mM phenylmethanesulfonyl fluoride (PMSF), and 0.5 mM dithiothreitol (DTT). Next, the precipitate was resuspended in 500 μL of fresh hypotonic buffer and allowed to swell on ice for 30 min. After homogenization in a Dounce homogenizer, nuclei were collected by centrifugation at 3300 × *g* for 15 min. After being washed with fresh hypotonic buffer, the nuclei were lysed and the expression of STAT5 and the phosphorylation level of STAT5 in the nucleus were tested by Western blot assay.

2.11. Animal experiments and grouping

A total of 48 BALB/C mice (aged 4–6 weeks and weighing 25 ± 3 g) were purchased from Laboratory Animal Research Center of Zhengzhou University (Zhengzhou, China). The mice were assigned into six groups (eight mice per group), including a blank group (without treatment), heparin group (injected with 0.0025 units/mL heparin), FGE2 group (injected with 20 ng/mL FGF2 and 0.0025 units/mL heparin), FGF2 + NC group (injected with 20 ng/mL FGF2 and HFSCs transduced with empty adenovirus vector), FGF2 + STAT5A-CA group (injected with 20 ng/mL FGF2 and HFSCs overexpressing pRKmSTAT5AHSFlag), and the FGF2 + STAT5A-DN group (injected with 20 ng/mL FGF2 and HFSCs overexpressing pRKmSTAT5A713Flag). Growth factor-reduced Matrigel (Becton Dickinson, San Jose, CA, USA) was adjusted to a concentration of 6.5 mg/mL with MEM, and mixed with 20 ng/mL FGF2 and 0.0025 units/mL heparin. Approximately 1×10^5 HFSCs infected with adenovirus vectors were then resuspended in 50 μL of PBS, and then administered to the mice subcutaneously (Lee et al., 2008). The Matrigel mixture (0.7 mL) was injected under the skin of the flank of the mice with a 21-G needle and permitted to solidify. Seven days later, the mice were euthanized with 3% pentobarbital sodium (No. P3761, Sigma-Aldrich, St Louis, MO, USA), and the Matrigel plugs and surrounding tissues were excised. The tissues were fixed in 10% neutral buffered paraformaldehyde. Paraffin-embedded tissues were sliced for immunohistochemistry.

2.12. Immunohistochemistry

The paraffin-embedded slices were placed in 3% H_2O_2 for 10 min and washed 3 times with distilled water (3 min each time). Next, the antigen was retrieved under high-pressure for 3 min, cooled down to room temperature in a water-bath, and then rinsed two times with 0.01 M PBS (pH = 7.4) (3 min each time). After being blocked with 10% normal goat serum blocking solution (CWbiotech, Ltd., Beijing, China) at room temperature for 20 min, the slices were incubated with the primary antibodies against STAT5 (ab227687, 1:100), vWF (ab6994, 1:200), VE-cadherin (ab232880, 1:100), CD31 (ab28364, 1:50), K15 (ab62335, 1:100) at 4 °C overnight. After being rinsed 3 times with PBS (3 min each time), the slices were incubated with biotin-labelled secondary antibody IgG (ab6566, 1:500) at 37 °C for 30 min. All antibodies used were purchased from Abcam Inc. (Cambridge, MA, USA). Afterwards, the slices were developed by 3 mL of diaminobenzidine (DAB; DA1010, Beijing Solarbio Science & Technology Co., Ltd., Beijing, China) for 5–10 min. The slices were then dehydrated in an ethanol series, cleared by xylene, and sealed with a neutral gum. Five fields were randomly selected from each slice for observation. Cell staining intensity scores ranged from 0 to 3 (no coloration, 0 points; light yellow, 1 point; brownish yellow, 2 points; tan, 3 points); the percentage of positive cells was scored from 0 to 4 (no positive-stained cell, 0 points; < 10%, 1 point; 10%–50%, 2 points,; 50%–80%, 3 points; > 80%, 4 points). Expression of each protein was represented by the total score of immunohistochemical staining, which was the product of the positive rate of staining cell score multiplied by the staining intensity score.

2.13. Statistical analysis

Statistical analysis was conducted using the SPSS 22.0 statistical software (IBM Corp, Armonk, NY, USA). The test of normal distribution and homogeneity of variance confirmed that all data conformed with the normal distribution. Measurement data in normal distribution were expressed as mean ± standard deviation. The comparison among multiple groups was analyzed by one-way analysis of variance (ANOVA), followed by a *post hoc* test. The data at different time points were compared by ANOVA with repeated measurement. A $p < 0.05$

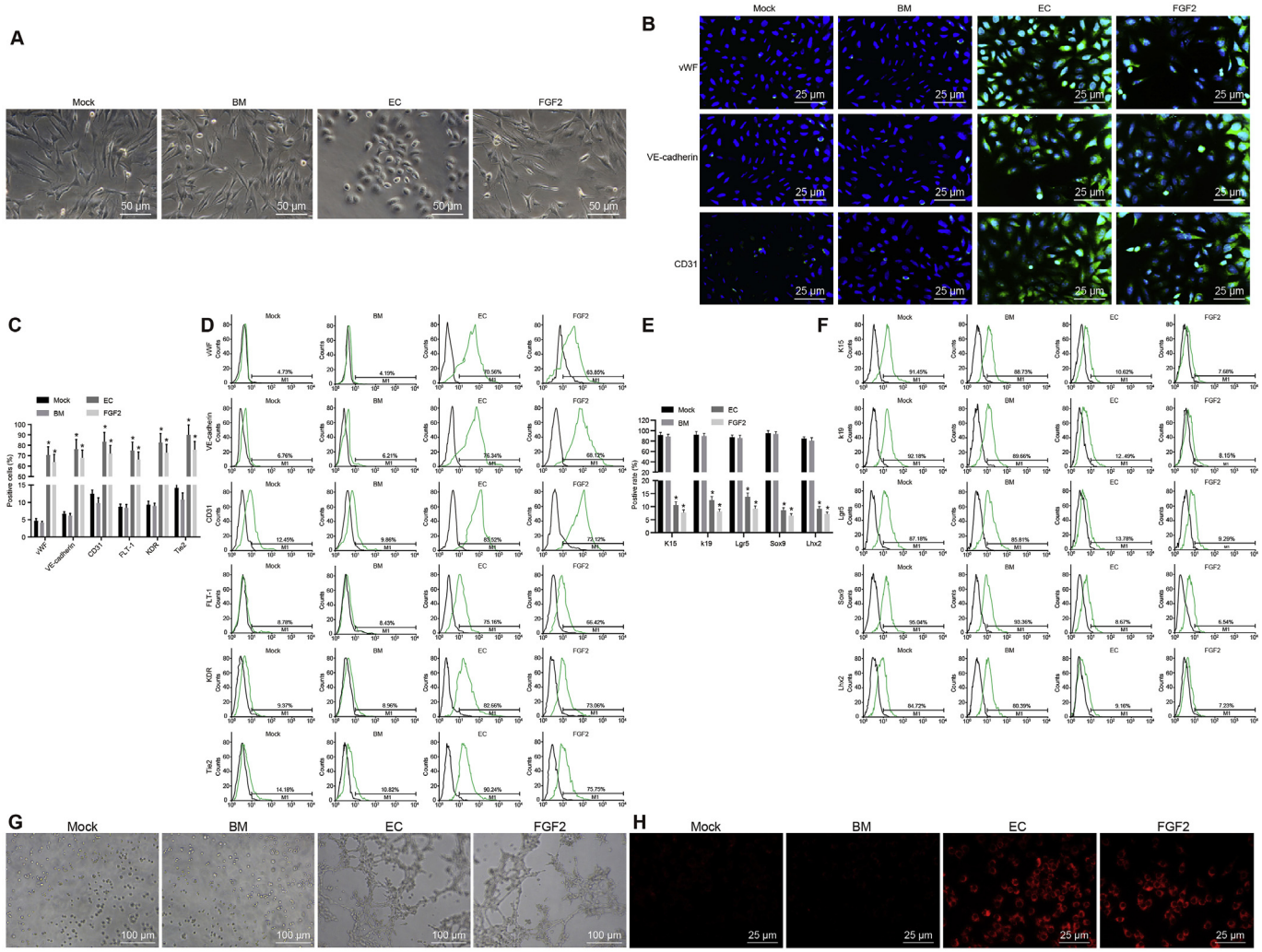

Fig. 1. The differentiation of HFSCs into ECs is facilitated by FGF2. Cell morphology of HFSCs with or without FGF2 treatment, with hUVECs as control (× 200) (A). Immunofluorescence staining to detect the expression of EC-specific markers, vWF, VE-cadherin and CD31 in HFSCs with or without FGF2 treatment, with hUVECs as control (× 400) (B). The expression of EC specific markers, vWF, ve-cadherin, CD31, FLT-1, KDR and Tie2 in HFSCs with or without FGF2 treatment, with hUVECs as control assessed by flow cytometry (C–D). The expression of human HFSCs specific markers, K15, K19, Lgr5, Sox9 and Lhx2 determined using flow cytometry (E–F). *In vitro* tube formation assay (scale bar = 500 μm) (G). Dil-acetylated LDL uptake assay (scale bar = 20 μm) (H). *$p < 0.05$ *vs.* the mock group. Statistical data were measurement data described as mean ± standard deviation. The comparisons among multiple groups were performed by one-way analysis of variance, and the experiment was repeated three times. HFSCs, human hair follicle stem cells; ECs, endothelial cells; FGF2, fibroblast growth factor 2; vWF, von Willebrand factor.

indicated that the difference was statistically significant.

3. Results

3.1. FGF2 promotes the differentiation of HFSCs into ECs

To explore the effect of FGF2 on the differentiation of HFSCs, HFSCs were treated with 10 nmol/L FGF2 and the morphology was observed seven days later, when the hUVECs of the EC group presented in cobblestone shapes. There was no marked difference in cell morphology between the mock group and the BM group, while the morphology of HFSCs in the FGF2 group was similar to that in the EC group (Fig. 1A). Immunofluorescence was conducted to determine expression of EC-specific markers, including vWF, VE-cadherin and CD31, none of which could be detected in the mock group. There was no noticeable difference in the EC-specific markers in the BM group compared with the mock group, while their expression was significantly upregulated in the FGF2 group, and to an even greater extent in the EC group (Fig. 1B). To confirm further the differentiation ability of HFSCs, we measured the expressions of vWF, VE-cadherin, CD31 FLT-1, KDR and Tie2 by flow cytometry. This consistently showed no obvious expression of the EC-specific markers in the mock group. Relative the mock group, there was no significant difference in the BM group ($p > 0.05$), while the expression of EC-specific markers in the FGF2 group was significantly up-regulated ($p < 0.05$), and to a greater extent in the EC group ($p < 0.01$) (Fig. 1C–D). Flow cytometry showed that the expression of HFSC specific markers K15, K19, Lgr5, Sox9, and Lhx2 did not differ between the mock group and the BM group ($p > 0.05$), while the expression of HFSCs-specific markers was significantly down-regulated in the FGF2 group ($p < 0.05$) and to a greater extent in the EC group ($p < 0.01$) (Fig. 1E–F). The tube formation assay showed that tube-like structures formed only in the EC and FGF2 groups ($p < 0.01$). Furthermore, the EC and macrophage property of Dil-acetylated LDL uptake (Costa et al., 2013) was absent in the mock and BM groups, while Dil-acetylated LDL uptake was distinctly observed in the EC and FGF groups (Fig. 1H). Taken together, FGF2 treatment promoted the differentiation of HFSCs into ECs, tube formation and Dil-acetylated LDL uptake.

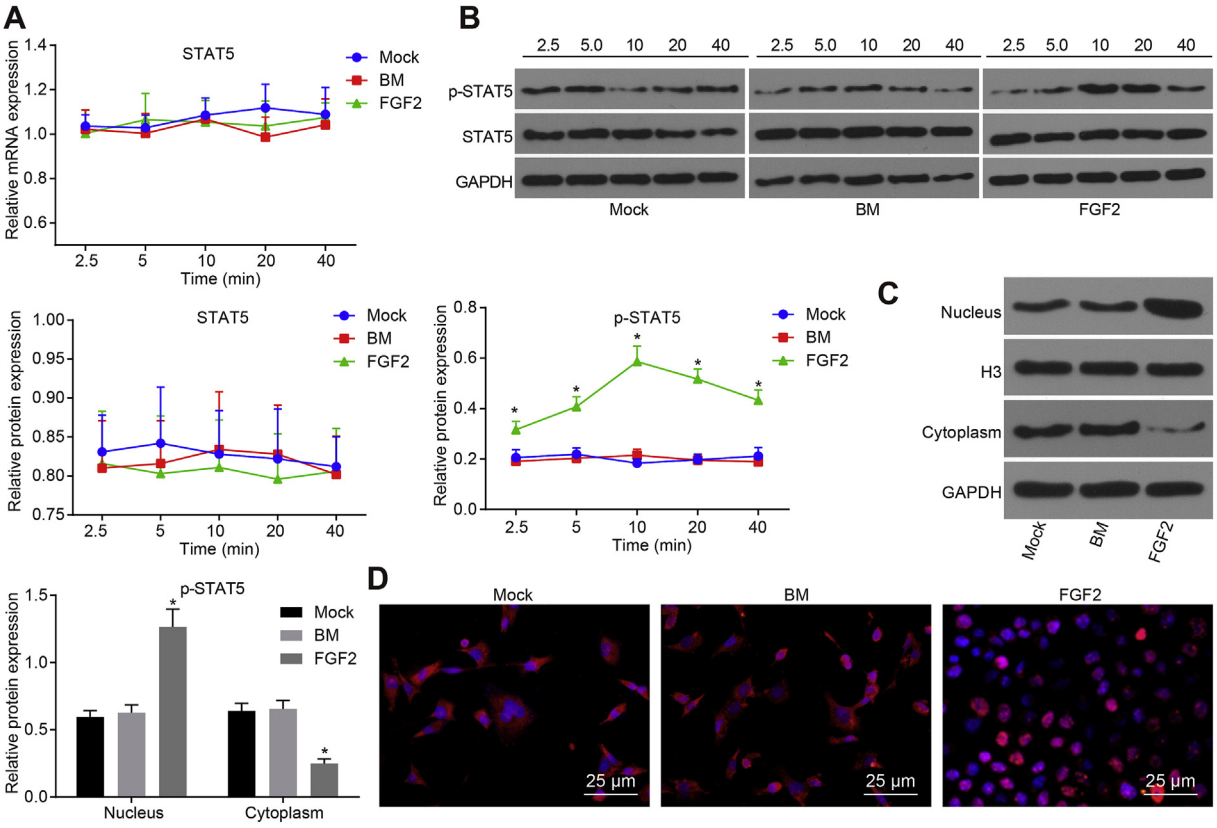

Fig. 2. FGF2 promotes STAT5 phosphorylation and induces nuclear translocation of phosphorylated STAT5 protein in HFSCs. The mRNA level of STAT5 after treatment with FGF2 measured by RT-qPCR (A). The protein level of STAT5 and the extent of STAT5 phosphorylation after treatment with FGF2 assessed by Western blot analysis (B). The extent of STAT5 phosphorylation in the nucleus and cytoplasm assessed by Western blot analysis (C). Immunofluorescence assay to detect the localization of p-STAT5 in HFSCs treated with FGF2 (× 400, scale bar = 25 μm) (D). *$p < 0.05$ *vs.* the mock group. Statistical data were measurement data described as mean ± standard deviation. The comparisons among multiple groups were performed by one-way analysis of variance, and the experiment was repeated three times. FGF2, fibroblast growth factor 2; STAT5, signal transducers and activators of transcription 5; HFSCs, human hair follicle stem cells; RT-qPCR, reverse transcription quantitative polymerase chain reaction.

3.2. FGF2 induces STAT5 phosphorylation and nuclear translocation of phosphorylated STAT5 in HFSCs

After treatment with FGF2, the expression of STAT5 was measured by RT-qPCR, and expression of STAT5 and the extent of its phosphorylation were determined by Western blot analysis. As depicted in Fig. 2A–B, there were no notable differences in STAT5 mRNA and protein expression among the mock, BM and FGF2 groups ($p > 0.05$). Neither was there any significant difference in STAT5 phosphorylation level between the mock and BM groups ($p > 0.05$). In comparison with the mock group, the phosphorylation level of STAT5 in the FGF2 group was significantly increased ($p < 0.05$), and at the 10th min, the extent of STAT5 phosphorylation induced by FGF2 reached its peak value (Fig. 2B). These results indicated that FGF2 can increase the extent of STAT5 phosphorylation in HFSCs.

STAT phosphorylation is necessary but not sufficient for STAT activation. STAT must translocate to the nucleus to function as a transcription factor, which can then activate downstream signaling (Eswarakumar et al., 2005). Therefore, we examined the presence of phosphorylated STAT5 in the nucleus in response to FGF2 treatment by Western blot analysis. We found that FGF2 treatment significantly increased the level of phosphorylated STAT5 in the nucleus ($p < 0.05$) (Fig. 2C). Finally, we measured the subcellular localization of phosphorylated STAT5 by immunofluorescence, which showed that phosphorylated STAT5 in the mock and BM groups was mainly localized in the cytoplasm, while phosphorylated STAT5 in the FGF2 group was mainly located in the nucleus (Fig. 2D). As a result, we conclude that FGF2 treatment led to nuclear translocation of phosphorylated STAT5 protein in HFSCs.

3.3. STAT5 is required for the differentiation of HFSCs promoted by FGF2

To examine the effect of STAT5 on FGF2-induced differentiation of HFSCs, HFSCs overexpressing STAT5A-CA (constitutive-active STAT5 mutant) or STAT5A-DN (dominant-negative STAT5 mutant) were treated by FGF2. Western blot analysis (Fig. 3A) showed that STAT5 protein expression was significantly enriched after HFSCs transduced with adenovirus vectors harboring STAT5A-CA (constitutive-active STAT5 mutant) or STAT5A-DN (dominant-negative STAT5 mutant) ($p < 0.5$), thus showing that these adenovirus vectors were successfully transduced into HFSCs. To immunostaining, as shown in Fig. 3B, phosphorylated STAT5 was distributed in the nucleus in the FGF2 + NV and FGF2 + STAT5A-CA groups, but was not visualized in the cells in the FGF2 + STAT5A-DN group, indicating that STAT5A-DN can block the nuclear translocation of STAT5 under FGF2 treatment.

Then, immunofluorescence studies showed that expression of the vWF, VE-cadherin and CD31 was remarkably elevated in FGF2 + NC group in contrast to the mock group ($p < 0.05$). However, when compared with the FGF2 + NC group, the expression of vWF, VE-cadherin and CD31 was increased in the FGF2 + STAT5-CA group but decreased in the FGF2 + STAT5-DN group ($p < 0.05$) (Fig. 3C). Meanwhile, flow cytometry showed that expression of the EC specific markers vWF, VE-cadherin, CD31, FLT-1, KDR and Tie2 was significantly higher in the FGF2 + NC group than in the mock group. In comparison with FGF2 + NC group, the marker expression was up-regulated in HFSCs overexpressing STAT5A-CA upon treatment with

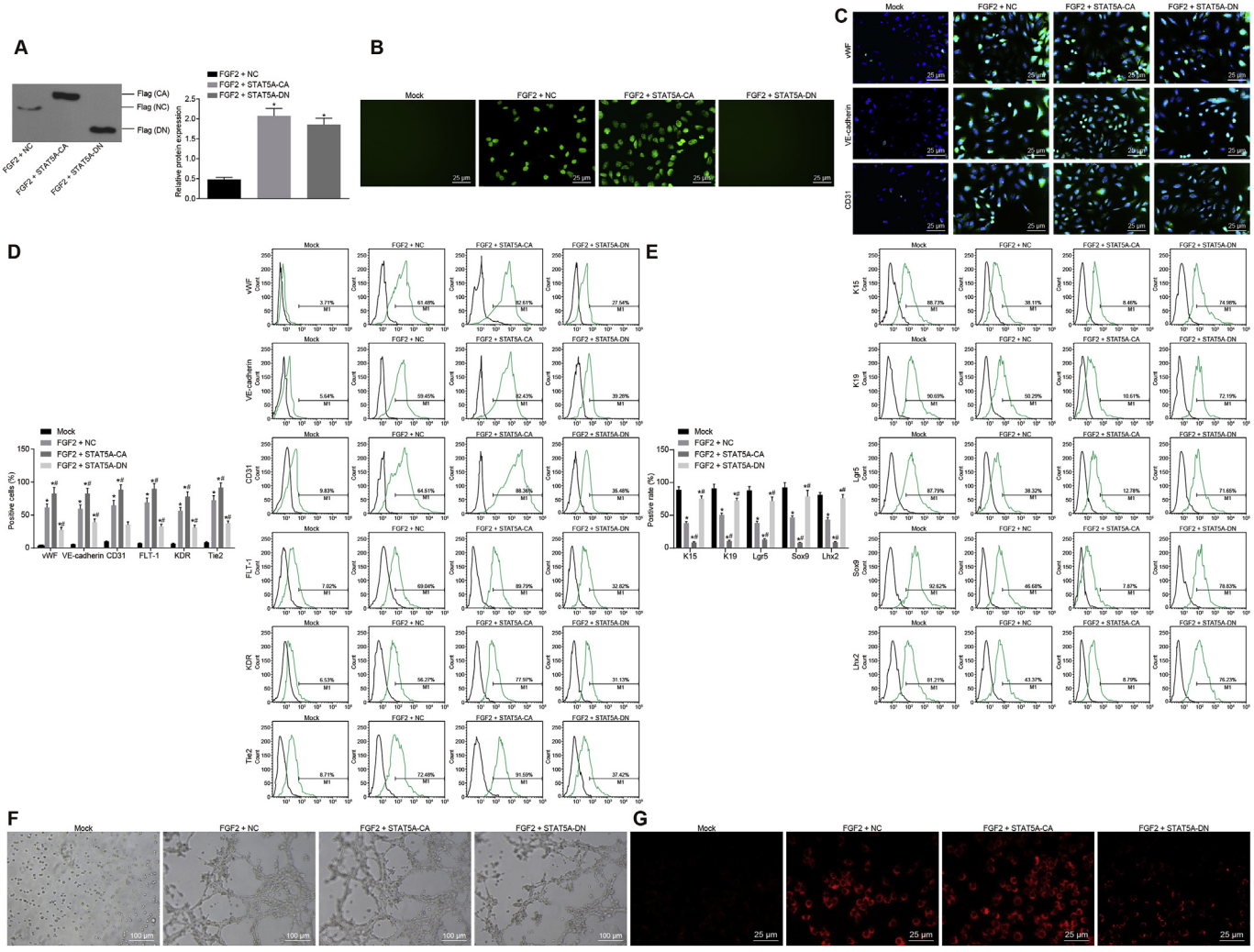

Fig. 3. STAT5 is necessary for the differentiation of HFSCs. Infection efficiency of the adenovirus vectors determined by Western blot assay (A). Immunofluorescence to examine the distribution of p-STAT5 in HFSCs overexpressing STAT5A-CA or STAT5A-DN (× 400) (B). Immunofluorescence staining to detect EC-specific markers, vWF, VE-cadherin and CD31 in HFSCs overexpressing STAT5A-CA or STAT5A-DN (× 400) (C). The expression of EC-specific markers vWF, VE-cadherin, CD31, FLT-1, KDR and Tie2 in HFSCs overexpressing STAT5A-CA or STAT5A-DN as detected by flow cytometry (D). The expression of the human HFSCs specific markers K15, K19, Lgr5, Sox9 and Lhx2 determined using flow cytometry (E). *In vitro* tube formation assay (scale bar = 500 μm) (F). Dil-acetylated LDL uptake assay (scale bar = 20 μm) (G). $^{*}p < 0.5$ *vs.* the mock group; $^{\#}p < 0.5$ *vs.* the FGF2 + NC group. Statistical data were measurement data described as mean ± standard deviation. The comparisons among multiple groups were performed by one-way analysis of variance, and the experiment was repeated three times. STAT5, signal transducers and activators of transcription 5; HFSCs, human hair follicle stem cells; ECs, endothelial cells; vWF, von Willebrand factor; FGF2, fibroblast growth factor 2; NC, negative control.

FGF2, but down-regulated in the similarly treated HFSCs overexpressing STAT5A-DN ($p < 0.05$) (Fig. 3D). Flow cytometry studies also showed that expression of HFSCs specific markers including K15, K19, Lgr5, Sox9 and Lhx2, was lower in the FGF2 + NC group than that in the mock group ($p < 0.05$). Compared with the FGF2 + NC group, the expression of the HFSCs specific markers was down-regulated in HFSCs overexpressing STAT5A-CA upon treatment of FGF2, but up-regulated in the similarly treated HFSCs overexpressing STAT5A-DN ($p < 0.05$) (Fig. 3E).

The *in vitro* tube formation assay did not reveal tube formation in the mock group. However, in contrast to the FGF2 + NC group, tube formation was conspicuous in the FGF2 + STAT5-CA group ($p < 0.01$), but less so in the FGF2 + STAT5-DN group (Fig. 3F). The dil-acetylated LDL uptake assay failed to detect uptake in the mock group, whereas Dil-acetylated LDL uptake was higher in the FGF2 +STAT5-CA group, but lower in the FGF2 + STAT5-DN group compared to that in the FGF2 + NC group (Fig. 3F). We conclude that activation of STAT5 is required in for differentiation of HFSCs and *in vitro* tube formation induced by FGF2.

3.4. FGF2 promotes in vivo differentiation of HFSCs into EC

We conducted animal experiments to explore further the *in vivo* role of FGF2 in promoting the differentiation of HFSCs. Immunofluorescence staining showed similar expression of the EC-specific markers, vWF, VE-cadherin, and CD31 (Fig. 4A) in the heparin and blank groups, while that was dramatically higher in the FGF2 group than in the blank group. The expression of HFSC-specific marker K15 in mouse tissue was significantly down-regulated in the FGF2 group when compared with that in the blank group (Fig. 4B). These results indicate that FGF2 promotes the differentiation of HFSCs into ECs *in vivo*.

3.5. The differentiation of HFSCs into ECs promoted by FGF2 is dependent on the activation of STAT5 in vivo

The requirement of STAT5 in FGF2-induced differentiation of HFSCs

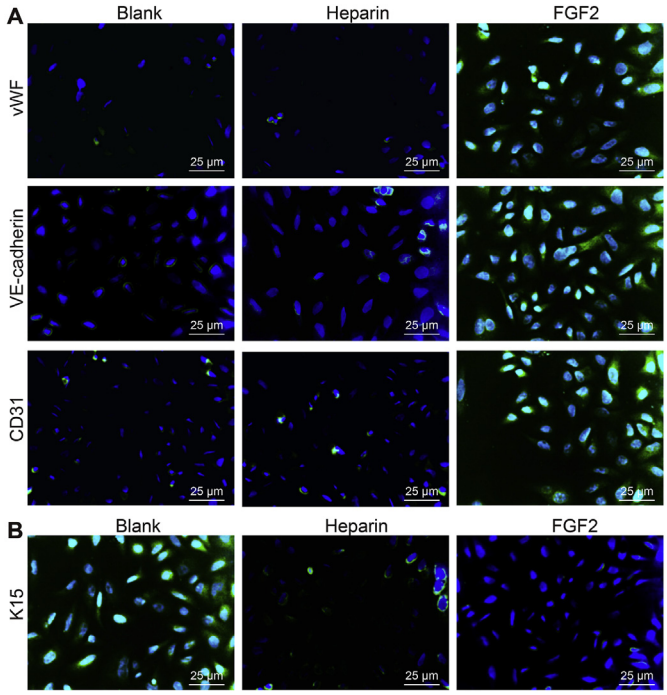

Fig. 4. The differentiation of HFSCs into ECs in mice is promoted by FGF2. Immunofluorescence staining of EC-specific markers, vWF, VE-cadherin and CD31 in mice injected with Heparin or FGF2 (× 400) (A). Immunofluorescence staining of HFSC-specific marker K15 in mice injected with Heparin or FGF2 (× 400) (B). The experiment was repeated 3 times. ECs, endothelial cells; FGF2, fibroblast growth factor 2; HFSCs, hair follicle stem cells.

was further analyzed *in vivo* in mice with subcutaneous injection with hHFSCs overexpressing STAT5A-CA or STAT5A-DN. The infection efficiency measured by Western blot analysis (Fig. 5A) showed dramatically elevated STAT5 expression in the FGF2 + STAT5A-CA and FGF2 + STAT5A-DN groups compared with that in the FGF2 + NC group ($p < 0.05$), suggesting that adenovirus vector transduction in both groups was successful. Then, immunohistochemical analysis in mouse tissue sections (Fig. 5B) showed significantly up-regulated STAT5 phosphorylation in the FGF2 + STAT5A-CA group compared with the FGF2 + NC group ($p < 0.05$), while that in the FGF2 + STAT5A-DN group was markedly down-regulated ($p < 0.05$). Next, immunohistochemistry for WF, VE-cadherin and CD31 (Fig. 5C) displayed that in comparison with the FGF2 + NC group, the expression of those EC-specific markers was significantly elevated in the FGF2 + STAT5A-CA group ($p < 0.05$), but reduced in the FGF2 + STAT5A-DN group ($p < 0.05$). Finally, immunohistochemical analysis showed down-regulated expression of the HFSC-specific marker K15 in the FGF2 + STAT5A-CA group ($p < 0.05$), but upregulated in the FGF2 + STAT5A-DN group as compared to the FGF2 + NC group ($p < 0.05$) (Fig. 5D). Moreover, examination of the resected Matrigel samples showed that angiogenesis was promoted in the FGF2 + STAT5-CA group, while the weakest angiogenic ability was found in the FGF2 + STAT5-DN group, as compared with that in the FGF2 + NC group (Fig. 5E). In conclusion, differentiation of HFSCs into ECs induced by FGF2 might rely on the activity of STAT5 *in vivo*.

4. Discussion

HFSCs have a substantial potential for applications in tissue engineering and regenerative medicine due to their easy accessibility along with the broad capacity for differentiation that they possess (Mistriotis and Andreadis, 2013). HFSCs are more likely to differentiate into ECs upon exposure to VEGF and FGF2 (bEGF) (Xu et al., 2014). It has been well documented that FGF2 is an extracellular matrix component required for supporting EC growth and promoting the formation of differentiated capillary tubes (Kinner et al., 2002). FGF2-mediated signaling is critical for the proliferation of hemangioblasts and thus positively regulates hematopoietic development. Several lines of evidence have indicated that FGF2 stimulates VEGF expression in ECs (Hyytiainen et al., 2004). The absence of FGF2 signaling leads to the loss of adherent and tight junctions, increased vascular leakiness, and disassembly of the existing vasculature. In this study, we focused on the mechanism underlying FGF2 modulation of the differentiation of HFSCs into ECs, both in murine models and in cultured hHFSCs. Our results support the proposition that recombinant human FGF2 contributes to enhanced HFSC differentiation. Additionally, we found the activation of STAT5 to be triggered in the differentiation process of HFSCs into ECs as induced by FGF2. Once in the nucleus, the phosphorylated STAT5 dimers bind to STAT5 responsive elements, modulating transcription of specific sets of genes. Upregulation of gene expression by STAT5 dimers has been observed for genes implicated in controlled cell growth and division, or cell proliferation.

One important finding in our study is that FGF2 promoted the differentiation of HFSCs into ECs. Here, we made use of vWF,VE-cadherin and CD31, which are widely recognized EC markers (Doan et al., 2014; Volz et al., 2017). In keeping with the present results, a previous study had demonstrated that FGF2 (bEGF) likewise induced their expression in hHFSCs (Zhang et al., 2014). K15 is known as one of the most distinctive molecular markers for HFSCs (Purba et al., 2014), and is used as a transit-amplifying cell marker related to the process of transformation of HFSCs to transit-amplifying cells (Shen et al., 2017). We propose that FGF2 could be developed as a biomarker for HFSC differentiation, given its role reported in a bioinformatics analysis as a regulator of differentiation of induced pluripotent stem cells toward hepatocytes (Lin et al., 2018). To sum up, the elevation in vWF, VE-cadherin and CD31 expression and reduction in K15 expression together suggest that FGF2 greatly contributed to the differentiation of HFSCs into ECs.

Another finding of our study was that in HFSCs, FGF2 induces the phosphorylation as well as nuclear translocation of STAT5. Previous studies show that treatment with FGF21, another member of the FGF family, extensively down-regulated the expression of growth factors such as PDGF, VEGF and CTGF by reducing the extent of STAT5 phosphorylation (Li et al., 2017). Besides, a tyrosine kinase growth factor receptor, FGFR-2, interacts with STAT-5 in the nuclei of breast cancer cells, in a manner correlating with the cytoplasmic and/or nuclear localization of STAT-5 (May et al., 2016). Moreover, other evidence supports that the differentiation of HFSCs into ECs promoted by FGF2 depends on the activation of STAT5 through overexpressing constitutively active STAT5 or dominant-negative STAT5 in HFSCs. A a member of the transcription factor family, STAT5 is a crucial modulator of cell differentiation and growth (Gianti and Zauhar, 2015). A previous study has shown that activated STATs could bind to particular DNA sequences in the promoter regions of different genes related to proliferation, differentiation and cell survival, that is to say, STAT5 could be functional when activated (Rondanin et al., 2014). The phosphorylated STAT5 hypersensitive response is related to a number of high-incidence diseases and signaling-related mutations (Padron et al., 2013). Various lines of evidence suggest that activation of STAT5 serves as a mesenchymal switch to induce anagen entry in the process of hair follicle cycling (Legrand et al., 2016). Furthermore, STAT5 activation promoted proliferation of intestinal epithelial stem cells (IESCs), and constitutively active STAT5 could facilitate $LGR5^+$ IESC self-renewal in both mouse and human stem cells (Gilbert et al., 2015). Partially consistent with results of our study, STAT5 was activated in response to FGF2 in mouse microvascular ECs and was confirmed to be an essential mediator for FGF-induced angiogenesis (Yang et al., 2009). Our murine model further supported the involvement of STAT5 activation in the FGF2-induced HFSC differentiation *in vivo*. All of these showed the

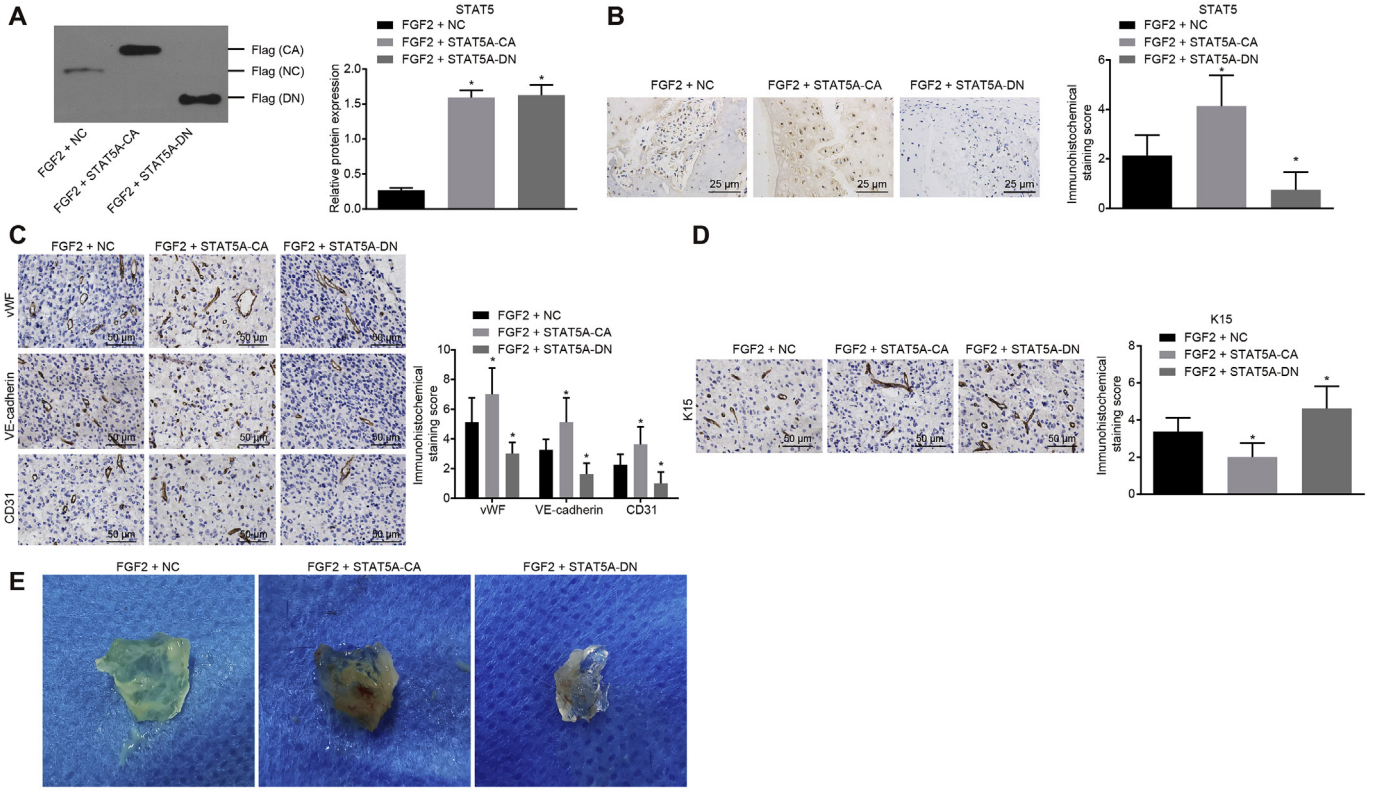

Fig. 5. STAT5 is essential for FGF2-induced differentiation of HFSCs into ECs in mice. Western blot was used to verify whether the adenovirus was successfully infected (A). Immunohistochemistry of the expression of STAT5 in mouse tissue slices after injection with the HFSCs infected with adenoviral vectors harboring STAT5A-CA or STAT5A-DN (× 400) (B). The expression of EC-specific markers, vWF, VE-cadherin and CD31 in mouse tissue slices detected by immunohistochemistry after injection with HFSCs infected with adenoviral vectors harboring STAT5A-CA or STAT5A-DN (× 200) (C). The expression of HFSC-specific marker, K15 in tissue slices detected by immunohistochemistry after injection with HFSCs infected with adenoviral vectors harboring STAT5A-CA or STAT5A-DN (× 200) (D). The angiogenesis of Matrigel was observed (E). *$p < 0.5$ *vs.* the FGF2 + NC group. Statistical data were measurement data described as mean ± standard deviation. The comparisons among multiple groups were performed by one-way analysis of variance, and the experiment was repeated three times. STAT5, signal transducers and activators of transcription 5; FGF2, fibroblast growth factor 2; HFSCs, hair follicle stem cells; ECs, endothelial cells; NC, negative control.

activation of STAT5 related to hair follicle and was of vital importance to the stem cells activities. It is reasonable to suppose that activation of STAT5 could contribute to the differentiation of HFSCs. However, STAT3 activation resulted in consumption of HF keratinocyte stem cells (KSC) together with proliferation stem cells, which indicated a significant role of STAT3 in the maintenance of KSCs (Rao et al., 2015). It remains a new and attractive research topic to verify which variants of STATs mediate response to FGF2.

In conclusion, FGF2 could promote the differentiation of HFSCs into ECs, entailing a phosphorylation level and nuclear translocation of HFSCs are increased in HFSCs. We expect that FGF2 presents a promising therapeutic target in studies of HFSC transplantation for treating various ischemic vascular diseases.

Funding

None.

Author contributions

Conception and design of research: BJC and YPZ; Performed experiments: YPZ and JDY; Analyzed data: BJC and XJL; Interpreted results of experiments: BJC and GWY; Prepared figures: JMW; Drafted manuscript: JDY and JMW; Edited and revised manuscript: XJL and GWY; Approved final version of manuscript: BJC, YPZ, XJL, JDY, JMW and GWY.

Declaration of competing interest

The authors have declared that no competing interests exist.

Acknowledgments

We extend our sincere appreciation to the reviewers for their helpful comments on this article.

References

Ayuk, S.M., Abrahamse, H., Houreld, N.N., 2016. The role of photobiomodulation on gene expression of cell adhesion molecules in diabetic wounded fibroblasts in vitro. J. Photochem. Photobiol., B 161, 368–374.

Beenken, A., Mohammadi, M., 2009. The FGF family: biology, pathophysiology and therapy. Nat. Rev. Drug Discov. 8, 235–253.

Call, M., Meyer, E.A., Kao, W.W., Kruse, F.E., Schlotzer-Schrehardt, U., 2018. Hair follicle stem cell isolation and expansion. Bio. Protoc. 8.

Chamorro-Jorganes, A., Araldi, E., Rotllan, N., Cirera-Salinas, D., Suarez, Y., 2014. Autoregulation of glypican-1 by intronic microRNA-149 fine tunes the angiogenic response to FGF2 in human endothelial cells. J. Cell Sci. 127, 1169–1178.

Costa, M., Sourris, K., Lim, S.M., Yu, Q.C., Hirst, C.E., Parkington, H.C., Jokubaitis, V.J., Dear, A.E., Liu, H.B., Micallef, S.J., Koutsis, K., Elefanty, A.G., Stanley, E.G., 2013. Derivation of endothelial cells from human embryonic stem cells in fully defined medium enables identification of lysophosphatidic acid and platelet activating factor as regulators of eNOS localization. Stem Cell Res. 10, 103–117.

Doan, C.C., Le, T.L., Hoang, N.S., Doan, N.T., Le, V.D., Do, M.S., 2014. Differentiation of umbilical cord lining membrane-derived mesenchymal stem cells into endothelial-like cells. Iran. Biomed. J. 18, 67–75.

Eswarakumar, V.P., Lax, I., Schlessinger, J., 2005. Cellular signaling by fibroblast growth factor receptors. Cytokine Growth Factor Rev. 16, 139–149.

Gianti, E., Zauhar, R.J., 2015. An SH2 domain model of STAT5 in complex with phosphopeptides define “STAT5 Binding Signatures”. J. Comput. Aided Mol. Des. 29,

451–470.
Gilbert, S., Nivarthi, H., Mayhew, C.N., Lo, Y.H., Noah, T.K., Vallance, J., Rulicke, T., Muller, M., Jegga, A.G., Tang, W., Zhang, D., Helmrath, M., Shroyer, N., Moriggl, R., Han, X., 2015. Activated STAT5 confers resistance to intestinal injury by increasing intestinal stem cell proliferation and regeneration. Stem Cell Rep. 4, 209–225.
Goetz, R., Mohammadi, M., 2013. Exploring mechanisms of FGF signalling through the lens of structural biology. Nat. Rev. Mol. Cell Biol. 14, 166–180.
Grigg, N., Schoenrock, A., Dick, K., Green, J.R., Golshani, A., Wong, A., Dehne, F., Tsai, E.C., Biggar, K.K., 2019. Insights into the suitability of utilizing brown rats (Rattus norvegicus) as a model for healing spinal cord injury with epidermal growth factor and fibroblast growth factor-II by predicting protein-protein interactions. Comput. Biol. Med. 104, 220–226.
Heidari, F., Yari, A., Rasoolijazi, H., Soleimani, M., Dehpoor, A., Sajedi, N., Joulai Veijouye, S., Nobakht, M., 2016. Bulge hair follicle stem cells accelerate cutaneous wound healing in rats. Wounds 28, 132–141.
Hyytiainen, M., Penttinen, C., Keski-Oja, J., 2004. Latent TGF-beta binding proteins: extracellular matrix association and roles in TGF-beta activation. Crit. Rev. Clin. Lab. Sci. 41, 233–264.
Kim, M.K., Park, H.J., Kim, S.R., Choi, Y.K., Bae, S.K., Bae, M.K., 2015. Involvement of heme oxygenase-1 in orexin-A-induced angiogenesis in vascular endothelial cells. KOREAN J. PHYSIOL. PHARMACOL. 19, 327–334.
Kinner, B., Zaleskas, J.M., Spector, M., 2002. Regulation of smooth muscle actin expression and contraction in adult human mesenchymal stem cells. Exp. Cell Res. 278, 72–83.
Lee, S.H., Chung, M.K., Sohn, Y.J., Lee, Y.S., Kang, K.S., 2008. Human hair follicle cells with the cell surface marker CD34 can regenerate new mouse hair follicles and located in the outer root sheath of immunodeficient nude mice. Int. J. Stem Cells 1, 70–81.
Legrand, J.M.D., Roy, E., Ellis, J.J., Francois, M., Brooks, A.J., Khosrotehrani, K., 2016. STAT5 activation in the dermal papilla is important for hair follicle growth phase induction. J. Investig. Dermatol. 136, 1781–1791.
Li, S., Guo, X., Zhang, T., Wang, N., Li, J., Xu, P., Zhang, S., Ren, G., Li, D., 2017. Fibroblast growth factor 21 ameliorates high glucose-induced fibrogenesis in mesangial cells through inhibiting STAT5 signaling pathway. Biomed. Pharmacother. 93, 695–704.
Lin, R., Wang, Y., Ji, K., Liu, Z., Xiao, S., Zhou, D., Chen, Q., Shi, B., 2018. Bioinformatics analysis to screen key genes implicated in the differentiation of induced pluripotent stem cells to hepatocytes. Mol. Med. Rep. 17, 4351–4359.
May, M., Mosto, J., Vazquez, P.M., Gonzalez, P., Rojas, P., Gass, H., Lanari, C., Molinolo, A.A., 2016. Nuclear staining of fgfr-2/stat-5 and runx-2 in mucinous breast cancer. Exp. Mol. Pathol. 100, 39–44.
Mistriotis, P., Andreadis, S.T., 2013. Hair follicle: a novel source of multipotent stem cells for tissue engineering and regenerative medicine. Tissue Eng. B Rev. 19, 265–278.
Nichane, M., Ren, X., Bellefroid, E.J., 2010. Self-regulation of Stat3 activity coordinates cell-cycle progression and neural crest specification. EMBO J. 29, 55–67.
Padron, E., Painter, J.S., Kunigal, S., Mailloux, A.W., McGraw, K., McDaniel, J.M., Kim, E., Bebbington, C., Baer, M., Yarranton, G., Lancet, J., Komrokji, R.S., Abdel-Wahab, O., List, A.F., Epling-Burnette, P.K., 2013. GM-CSF-dependent pSTAT5 sensitivity is a feature with therapeutic potential in chronic myelomonocytic leukemia. Blood 121, 5068–5077.
Purba, T.S., Haslam, I.S., Poblet, E., Jimenez, F., Gandarillas, A., Izeta, A., Paus, R., 2014. Human epithelial hair follicle stem cells and their progeny: current state of knowledge, the widening gap in translational research and future challenges. Bioessays 36, 513–525.
Quan, R., Du, W., Zheng, X., Xu, S., Li, Q., Ji, X., Wu, X., Shao, R., Yang, D., 2017. VEGF165 induces differentiation of hair follicle stem cells into endothelial cells and plays a role in in vivo angiogenesis. J. Cell Mol. Med. 21, 1593–1604.
Rao, D., Macias, E., Carbajal, S., Kiguchi, K., DiGiovanni, J., 2015. Constitutive Stat3 activation alters behavior of hair follicle stem and progenitor cell populations. Mol. Carcinog. 54, 121–133.
Rondanin, R., Simoni, D., Romagnoli, R., Baruchello, R., Marchetti, P., Costantini, C., Fochi, S., Padroni, G., Grimaudo, S., Pipitone, R.M., Meli, M., Tolomeo, M., 2014. Inhibition of activated STAT5 in Bcr/Abl expressing leukemia cells with new pimozide derivatives. Bioorg. Med. Chem. Lett 24, 4568–4574.
Seo, H.R., Jeong, H.E., Joo, H.J., Choi, S.C., Park, C.Y., Kim, J.H., Choi, J.H., Cui, L.H., Hong, S.J., Chung, S., Lim, D.S., 2016. Intrinsic FGF2 and FGF5 promotes angiogenesis of human aortic endothelial cells in 3D microfluidic angiogenesis system. Sci. Rep. 6, 28832.
Shen, Q., Yu, W., Fang, Y., Yao, M., Yang, P., 2017. Beta-catenin can induce hair follicle stem cell differentiation into transit-amplifying cells through c-myc activation. Tissue Cell 49, 28–34.
Tam, W.F., Hahnel, P.S., Schuler, A., Lee, B.H., Okabe, R., Zhu, N., Pante, S.V., Raffel, G., Mercher, T., Wernig, G., Bockamp, E., Sasca, D., Kreft, A., Robinson, G.W., Hennighausen, L., Gilliland, D.G., Kindler, T., 2013. STAT5 is crucial to maintain leukemic stem cells in acute myelogenous leukemias induced by MOZ-TIF2. Cancer Res. 73, 373–384.
Volz, A.C., Huber, B., Schwandt, A.M., Kluger, P.J., 2017. EGF and hydrocortisone as critical factors for the co-culture of adipogenic differentiated ASCs and endothelial cells. Differentiation 95, 21–30.
Woo, W.M., Oro, A.E., 2011. SnapShot: hair follicle stem cells. Cell 146, 334–334 e332.
Xu, Z.C., Zhang, Q., Li, H., 2014. Differentiation of human hair follicle stem cells into endothelial cells induced by vascular endothelial and basic fibroblast growth factors. Mol. Med. Rep. 9, 204–210.
Yang, X., Qiao, D., Meyer, K., Friedl, A., 2009. Signal transducers and activators of transcription mediate fibroblast growth factor-induced vascular endothelial morphogenesis. Cancer Res. 69, 1668–1677.
Yang, X., Qiao, D., Meyer, K., Pier, T., Keles, S., Friedl, A., 2012. Angiogenesis induced by signal transducer and activator of transcription 5A (STAT5A) is dependent on autocrine activity of proliferin. J. Biol. Chem. 287, 6490–6502.
Zhang, H., Qiu, J., Ye, C., Yang, D., Gao, L., Su, Y., Tang, X., Xu, N., Zhang, D., Xiong, L., Mao, Y., Li, F., Zhu, J., 2014. ROR1 expression correlated with poor clinical outcome in human ovarian cancer. Sci. Rep. 4, 5811.
Zhang, H., Zhao, H., Qiao, J., Zhang, S., Liu, S., Li, N., Lei, X., Ning, L., Cao, Y., Duan, E., 2016. Expansion of hair follicle stem cells sticking to isolated sebaceous glands to generate in vivo epidermal structures. Cell Transplant. 25, 2071–2082.